Anthony J. Gannon

Theodor W. von Backström
e-mail: twvb@ing.sun.ac.za

Department of Mechanical Engineering,
University of Stellenbosch,
Private Bag X1,
Matieland 7602, South Africa

Solar Chimney Cycle Analysis With System Loss and Solar Collector Performance

An ideal air standard cycle analysis of the solar chimney power plant gives the limiting performance, ideal efficiencies and relationships between main variables. The present paper includes chimney friction, system, turbine and exit kinetic energy losses in the analysis. A simple model of the solar collector is used to include the coupling of the mass flow and temperature rise in the solar collector. The method is used to predict the performance and operating range of a large-scale plant. The solar chimney model is verified by comparing the simulation of a small-scale plant with experimental data.
[S0199-6231(00)00503-7]

Introduction

The solar chimney is a simple renewable energy source consisting of three main components, a solar collector, chimney and turbine. Air is heated by the greenhouse effect under the glass collector. This hot air, less dense than the surroundings, rises up the chimney at the center of the collector. At the base of the chimney an electricity generating turbine is driven by the rising air. Economic and feasibility studies have been performed [1,2].

Ideal Air Standard Cycle Analysis

There have been various analyses of the solar chimney [2,3], and an ideal air standard cycle analysis [4], included here for clarity (Fig. 1). While simple it is rigorous and determines a cycle's limiting efficiency as all components are assumed to be ideal and all processes loss free. Other assumptions are: the working fluid is dry air, considered an ideal gas with constant specific heat capacity. The only heat flow in the system is the net gain by the air in the collector. The mass flow in the system is constant and inlet and outlet atmospheric conditions are ideal.

Figure 2 shows the solar chimney cycle, while Table 1 clarifies the processes and lists the similarities to the gas turbine cycle. These similarities greatly simplify the analysis as existing gas turbine theory can be used [5]. The aim of the analysis is to find a relationship between the plant performance and variables such as chimney height and collector temperature rise.

The plant thermal efficiency is defined as,

$$\eta = \frac{\text{Shaft Power Out}}{\text{Solar Power In}} \tag{1}$$

where the denominator, the available solar power is,

$$P_{solar} = \dot{m} c_p (T_3 - T_2) = \dot{m} c_p \Delta T_{23} \tag{2}$$

Not all of the power from expansion 3–4 is available as some of it is required to lift the air up the chimney (3te-4) [6],

$$P_{3-4} = \dot{m} c_p (T_3 - T_4) \tag{3}$$

$$P_{3te\text{-}4} = \dot{m} c_p (T_{3te} - T_4) = \dot{m} \Delta h = \dot{m} g \Delta z \tag{4}$$

and an adiabatic lapse rate [7]

$$-\frac{dT}{dz} = \frac{g}{c_p} \tag{5}$$

the enthalpy reduction from 3te-4 is the same as from 1′–2

$$\Delta h = g \Delta z = c_p (T_2 - T_{1'}) \tag{6}$$

Resulting in a shaft power output of,

$$P_{shaft} = \dot{m} c_p (T_3 - T_4) - \dot{m} c_p (T_2 - T_{1'}) \tag{7}$$

Substituting Eqs. (2) and (7), the ratio, $c = T_2/T_{1'} = T_3/T_4$ for the ideal isentropic gas process and the relation of Eq. (6) all into (1) the ideal plant efficiency is written as,

$$\eta = 1 - \frac{1}{c} = \frac{g \Delta z}{c_p T_2} \tag{8}$$

In a similar way the specific power normalized with respect to the mass flow and inlet temperature T_2 is defined as,

$$P_2^* = \frac{P_{shaft}}{\dot{m} c_p T_2} \tag{9}$$

where substitution of c leads to the intermediate step of,

$$P_2^* = \left\{1 - \frac{1}{c}\right\} \left\{\frac{T_3 - T_2}{T_2}\right\} \tag{10}$$

and using Eq. (6) leads to,

$$P_2^* = \left\{\frac{g \Delta z}{c_p T_2}\right\} \left\{\frac{\Delta T_{23}}{T_2}\right\} \tag{11}$$

Equations (8) and (11) represent the upper limits of the solar chimney performance as they are derived from the ideal cycle analysis. The efficiency (Eq. (8)) is proportional to chimney

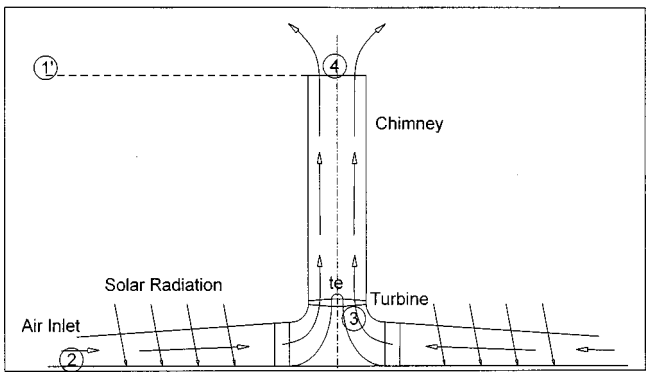

Fig. 1 Solar chimney schematic

Contributed by the Solar Energy Division of THE AMERICAN SOCIETY OF MECHANICAL ENGINEERS for publication in the ASME JOURNAL OF SOLAR ENERGY ENGINEERING. Manuscript received by the ASME Solar Energy Division, Dec. 1999; final revision, Jul. 2000. Associate Technical Editor: T. Mancini.

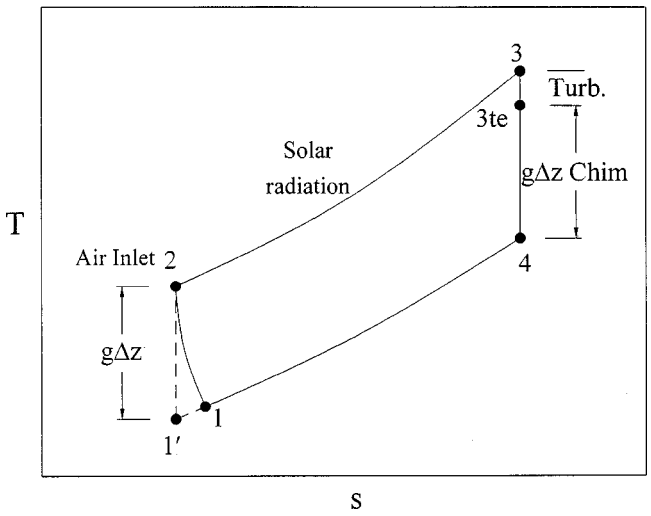

Fig. 2 Temperature-entropy diagram for air standard cycle analysis

Table 1 Comparison between solar chimney and gas turbine cycle

Process no.	Gas turbine	Solar chimney
1–2	Compressor	Atmospheric lapse rate
2–3	Combustor	Solar collector
3–4	Turbine	Turbine and chimney

Table 2 Efficiencies and specific power output from ideal air standard cycle analysis

Δz [m] ⇓	η [%] ⇓	$P_2^*(\times 10^3)$ for various ΔT_{23}				
		5	10	15	20	30
1500	4.83	0.796	1.593	2.389	3.185	4.778
1000	3.22	0.531	1.062	1.593	2.124	3.185
500	1.61	0.265	0.531	0.796	1.062	1.593

height and inversely so to inlet temperature T_2. The inlet conditions are dependent on climatic conditions and so plant efficiency is controlled solely by the chimney height. Assuming $T_2 = 303.2$ K, the following efficiencies and specific powers are the upper limits for the given chimney heights.

Inclusion of Losses

In the real plant losses will occur in each of the components. Two assumptions are made, the first that the total pressure remains constant under the glass collector as air is likely to leak in. Practically this would result in a lower temperature rise, ΔT_{23}. The second is that all kinetic energy is lost at the exit as it would be difficult to construct a diffuser at the top of the chimney. The temperature entropy diagram is modified to include component losses.

Figure 3 shows the 3 main components of the expansion process, namely the turbine, chimney and kinetic energy loss at the exit. The turbine efficiency is defined as,

$$\eta_{turb} = \frac{T_{03} - T_{03te}}{T_{03} - T_{03te'}} \tag{12}$$

Apart from the work required to lift the air up the chimney further work is required to overcome the internal friction of the chimney mainly due to internal bracing and to a lesser extent wall friction. Represented by *k*, this is expressed as a fraction of the exit kinetic energy,

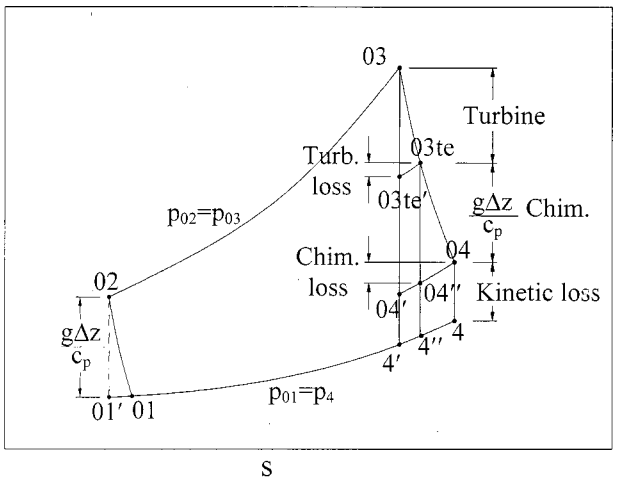

Fig. 3 Temperature-entropy diagram for air standard cycle analysis with system losses

$$k = \frac{T_{04} - T''_{04}}{T_{04} - T_4} \tag{13}$$

In general the exit velocity is not uniform and using the mean is simpler. Calculation of the exit kinetic energy using the mean is not correct so a factor, α, is introduced allowing the mean to be used but giving the correct exit kinetic energy. In the following definition of α, over bars denote the mean values.

$$\alpha = \frac{KE}{\overline{KE}} = \frac{\int (\rho C_{z4}) \frac{1}{2} C_{z4}^2 dA}{(\rho \overline{C_{z4}}) \frac{1}{2} \overline{C_{z4}^2} A} \tag{14}$$

The entire expansion efficiency is defined as

$$\eta_{\exp} = \frac{(T_{03} - T_4)}{(T_{03} - T'_4)} \tag{15}$$

Efficiency and Specific Power Output. Using the definition of efficiency from Eq. (1) and through inspection of Fig. 3 to take kinetic energy loss (04-4) into account plant efficiency is,

$$\eta = \frac{\eta_{\exp}(T_{03} - T'_4) - (T_{03te} - T_{04}) - (T_{04} - T_4)}{(T_{03} - T_{02})} \tag{16}$$

from which the following expressions for efficiency and specific power can be written,

$$\eta = \left(\frac{g\Delta z}{c_p T_{02}}\right)\left[\frac{\eta_{\exp}(T_{02} + \Delta T_{23}) - T_{02}}{\Delta T_{23}}\right] - \alpha \frac{\overline{C_{z4}^2}}{2 c_p \Delta T_{23}} \tag{17}$$

$$P_2^* = \left(\frac{g\Delta z}{c_p T_{02}}\right)\left(\frac{\eta_{\exp}(T_{02} + \Delta T_{23}) - T_{02}}{T_{02}}\right) - \alpha \frac{\overline{C_{z4}^2}}{2 c_p T_{02}} \tag{18}$$

When $\eta_{\exp} = 1$ and $C_{z4} = 0$ then Eqs. (17) and (18) simplify to Eqs. (8) and (11) respectively.

Operating Range. The solar chimney can operate between two extremes of zero power output. The first is simply when there is a zero turbine temperature drop resulting in a large mass flow. The second is when there is a near zero mass flow caused by a high turbine temperature drop. As before this is illustrated in a temperature entropy diagram showing the condition (Fig. 4).

The limiting turbine temperature drop is defined as,

$$\Delta T_{turb\,\lim} = (T_{03} - T'_{03te}) = \frac{(T_{03} - T_4) - (T_{03te} - T_4)}{\eta_{turb}} \tag{19}$$

By making the following substitutions into Eq. (19),

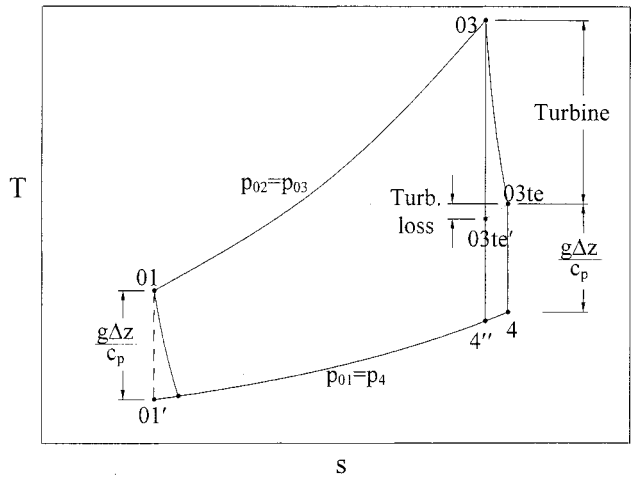

Fig. 4 Temperature-entropy diagram for air standard cycle analysis with system losses for limiting turbine temperature drop

$$T_4 = T_{03te}(T_4'/T_{03te}')$$
$$T_{03te} = T_{03} - \eta_{turb}(T_{03} - T_{03te}') = T_{03} - \eta_{turb}(\Delta T_{turb\ \lim}) \quad (20)$$
$$T_{03te}' = T_{03} - (T_{03} - T_{03te}') = T_{03} - \Delta T_{turb\ \lim}$$
$$\frac{g\Delta z}{c_p} = T_{03te} - T_4$$

an implicit expression for $\Delta T_{turb\ \lim}$ results,

$$\Delta T_{turb\ \lim} = \frac{1}{\eta_{turb}}\left[\left(T_{03} - T_4'\frac{T_{03} - \eta_{turb}\Delta T_{turb\ \lim}}{T_{03} - \Delta T_{turb\ \lim}}\right) - \frac{g\Delta z}{c_p}\right] \quad (21)$$

Equation (21) can be written in standard quadratic form with a, b and c being the standard coefficients. The physically realistic solution is,

$$\Delta T_{turb\ \lim} = \frac{-b - \sqrt{b^2 - 4ac}}{2a} \quad (22)$$

Output Power. The total output power is a function of the plant size, environmental conditions and a specified turbine temperature drop and is calculated by multiplying Eq. (18) as follows,

$$P = \dot{m} c_p T_{02} P_2^* \quad (23)$$

Inspection of Eqs. (18) and (23) shows that the exit velocity, C_{z4} and system mass flow are required. The mass flow is a function of chimney area and C_{z4} and ρ_4,

$$\dot{m} = \rho_4 C_{z4} A \quad (24)$$

For both C_{z4} and ρ_4, the exit temperature T_4 is required,

$$\rho_4 = \frac{p_4}{RT_4} \quad (25)$$

$$\overline{C_{z4}} = \sqrt{2c_p(T_{04} - T_4)/\alpha} \quad (26)$$

From Fig. 3 the following three temperature ratios can be written,

$$\frac{T_4}{T_{04}} = \frac{T_4'}{T_{04}'}; \quad \frac{T_{04}'}{T_{03te}'} = \frac{T_{04}''}{T_{03te}}; \quad T_{04}'' = T_{04} - k(T_{04} - T_4); \quad (27)$$

Once again this leads to an implicit equation for T_4,

$$T_4 = \frac{T_{04}T_4'T_{03te}}{T_{03te}'[T_{04} - k(T_{04} - T_4)]} \quad (28)$$

which can be re-written in standard quadratic form leading to the solution,

$$T_4 = \frac{-b + \sqrt{b^2 - 4ac}}{2a} \quad (29)$$

The exit pressure, p_4 is the last term needed and assuming an adiabatic atmospheric lapse rate it can be written as,

$$\frac{p_4}{p_{03}} = \frac{p_{01}}{p_{02}} = \left(\frac{T_{01}}{T_{02}}\right)^{\gamma/\gamma-1} \Rightarrow p_4 = p_{02}\left(1 - \left\{\frac{g\Delta z}{c_p T_{02}}\right\}\right)^{\gamma/\gamma-1} \quad (30)$$

Solar Collector Model

The last major component to be included in the analysis is the solar collector which supplies input heat to the system. In the collector there is a strong coupling between the mass flow and temperature rise of the air ($Q_{air} = mc_p\Delta T$). Previous analyses of the solar chimney have not taken this into account and use a gas turbine approach of plotting performance along lines of constant collector temperature rise, ΔT_{23}. A more useful result would be plant power output along lines of constant inlet radiation. These two approaches lead to very different predictions of design point operation as shown in Table. The collector model gives the relationship between G and Q_{air}.

Solar Collector Model. There are three basic assumptions used in the model and these are: 1) steady state conditions 2) No evaporation takes place under the collector and 3) the vertical temperature profile of the collector air is constant. Figure 5 shows the annular control volume used to find the net heat gain of the air through each section of the collector [8–10].

The following energy balance equation can be written to find the heat gain by the air in the control volume,

$$dH_{\dot{m}} = (dG - dG_{loss}) + (dQ_{loss} + dQ_{sto}) \quad (31)$$

This can be expanded by substituting the normal equations for radiation and convection loss to the atmosphere as well as conduction loss into the soil. The temperature rise through each control volume by the air is,

$$\frac{dT_{air}}{dr} = \frac{2\pi r}{\dot{m}c_p}\left[\tau_{in}e_{surf}G - \left\{\tau_{out}e_{surf}\sigma(T_{surf}^4 - T_{atm}^4) + h_{gli}(T_{air} - T_{gli}) + \frac{k_{gro}}{L_{gro}}(T_{surf} - T_{sto})\right\}\right] \quad (32)$$

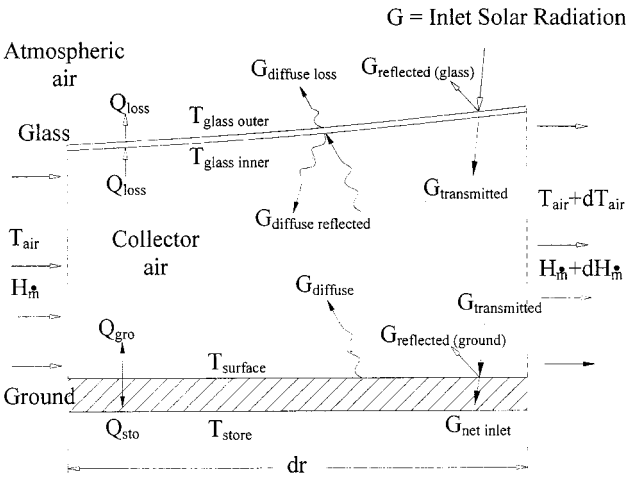

Fig. 5 Detail of control colume of solar collector showing nomenclature for temperatures, heat, mass and radiation flow

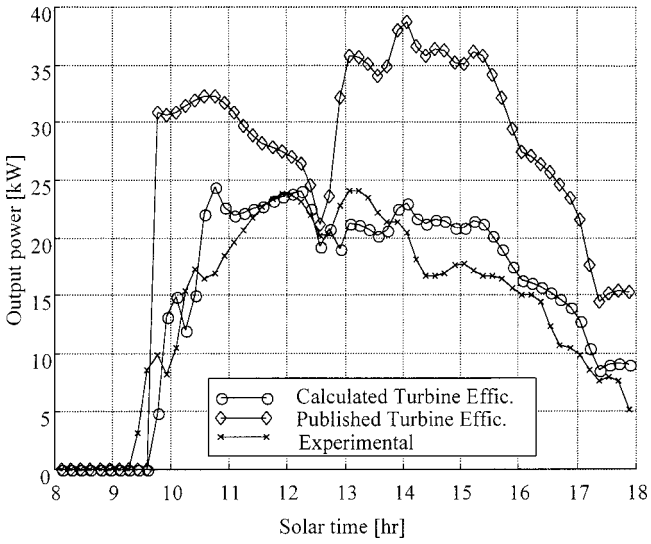

Fig. 6 Comparison of simulated and experimental results from Manzares, Spain

Three further heat flow equations, the ground surface (33), glass inner surface (34) and glass outer surface (35) are needed to calculate the temperatures for use in Eq. (32).

$$\tau_{in}e_{surf}G=\tau_{out}e_{surf}\sigma(T_{surf}^4-T_{atm}^4)+h_{surf}(T_{surf}-T_{air})+\frac{k_{gro}}{L_{gro}}(T_{surf}-T_{sto}) \quad (33)$$

$$h_{gli}(T_{air}-T_{gli})=\frac{k_{glass}}{L_{glass}}(T_{gli}-T_{glo}) \quad (34)$$

$$\frac{k_{glass}}{L_{glass}}(T_{gli}-T_{glo})=h_{glo}(T_{glo}-T_{atm}) \quad (35)$$

With the inlet conditions to the collector being known Eq. (32) being a one dimensional differential equation can be solved numerically. For a given mass flow the temperature rise ΔT_{23} can be found.

Manzanares Simulation

To verify the solar chimney model a small-scale plant is simulated [3] and the results compared with experimental readings. Assuming steady state conditions for the air is accurate but not so for the soil temperatures. A simple one dimensional finite difference time marching scheme was used to model the soil [8] and it was found to improve the transient simulation of the Manzanares plant significantly. The plant in Manzanares had a chimney of 194.6 m high, 10 m in diameter and a solar collector of radius 122 m. Figure 6 above compares simulated results and experimental results using the environmental data of [11] published for a sample day (02-09-82) where the maximum inlet radiation was 850 W/m^2.

It can be seen that there are two set of simulated results, the first is using the quoted turbine efficiency, assuming it stays constant. Inspection of the measured turbine pressure drop vs the power output shows that this is not the case and calculating the turbine efficiency improves the results. The simulation tends to overestimate the power output in the morning and afternoon, this is hoped to be improved by taking into account reflection due to the sun's low angle. The dip in midday output is thought to be due to incorrect turbine modeling. The power outputs are in the correct range and so the model can be used with reasonable certainty in predicting the power output of a full-scale plant.

Simulation of Full Scale Plant

The model developed is used to simulate a full scale solar chimney. Table 3 shows the size and inlet conditions used for the simulation. Values used for the various material constants can be found in [8] but these are similar to the nominal values found in most texts.

Power Output. Figure 7 shows that the plant power output at a certain inlet radiation level is not constant but can be varied by changing the turbine temperature drop. The two extreme conditions that result in zero mass flow can be clearly seen. It is also evident that there is a maximum power condition as shown. What is also indicated is a limiting power line, this is due to the maximum power output of the generator. It can also be seen that the design power can be reached at a reasonable inlet radiation level.

The reason for indicating the region to the left of the max power line as the 'ideal operating region' needs further discussion. At an inlet radiation of say 800 W/m^2 with power limited to 200 MW there are two possible operating points.

The first at a higher mass flow to the right of the maximum power line would be reducing power output by increasing the kinetic energy losses at the exit. The temperature in the solar collector would also be reduced thus reducing the effectiveness of any thermal storage.

The second point, to the left, is at a lower mass flow rate decreasing the power output by increasing the temperature and thus heat loss in the solar collector. As mentioned part of this ''loss'' is into the ground but this heat would be used later in the day as the air temperature cools and inlet radiation decreases. In practice the plant would probably be operate along the maximum power line until the limiting power was reached. The mass flow would then be limited to control the power output.

Turbine Requirements. To be able to generate power an efficient turbine is required and to design this accurate predictions

Table 3 Dimensions and inlet conditions

	Full-scale	Manzanares
Chimney diameter	160 m	10 m
Chimney height	1500 m	195 m
Chimney constant k	1	
Design power	200 MW	50 kW
Collector inlet press (p_2)	90 000 Pa	
Collector inlet temp. (T_2)	303.2 K	
Turbine efficiency	80%	
Exit constant α	1.1058	

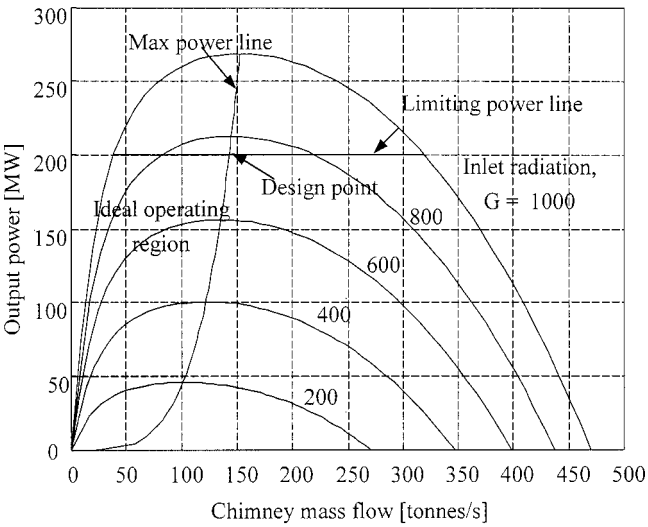

Fig. 7 Power output vs. mass flow along line of constant inlet radiation

Table 4 Turbine design point prediction

	Lines of constant radiation [W/m^2]	Lines of constant temperature [K]
ΔT_{23} [K]	37.4	24.01
ΔP_{turb} [Pa]	1597	749
Mass flow [t/s]	143.1	318.9

of mass flow and pressure drop are required. It is assumed that the turbine will operate along the maximum power line at lower inlet radiation levels and then to the left of this along the limiting power line at higher levels. In previous analyses of the solar chimney a graph similar to Fig. 7 has been produced but plotting power output along lines of constant temperature (the gas turbine approach as mentioned earlier). The difference in turbine operating predictions at the indicated design point using these two methods is shown in Table 4.

Conclusion

The ideal air standard cycle analysis while simple to perform is a powerful tool as it quickly allows the upper limits of a cycle's performance to be calculated. In the solar chimney project this is important so that initial feasibility of the plant can be quickly calculated. The inclusion of the main system losses of turbine efficiency, chimney friction and exit kinetic energy loss allow for more realistic predictions of plant power output to be found. The final step of the analysis is the inclusion of the solar collector and is important due to the strong coupling of mass flow and temperature drop.

Care must be taken when predicting the operating range of the solar chimney. Using a traditional approach, plotting power output along lines of constant power and not including the solar collector in the analysis could result in an inaccurate prediction of the operating region. Plotting the power output along lines of constant inlet radiation better represents the performance of the solar chimney, as it simulates the actual conditions better. Accurate prediction of the operating region will result in a more efficient turbine design. The analytical model developed showed good agreement with the experimental results of the small-scale plant built in Manzanares allowing it to be used reliably in the prediction of the output of a full-scale plant.

Nomenclature

Cycle Analysis

- a = quadratic constant
- A = area
- b = quadratic constant
- c = quadratic constant
- c_p = specific heat capacity
- C = velocity
- g = gravitational constant
- h = enthalpy
- K = chimney loss coeff.
- $\dot{m}$ = mass flow
- KE = kinetic energy
- p = pressure
- P = power
- R = gas constant
- T = temperature
- z = vertical height
- α = kinetic energy coeff.
- γ = gas constant
- η = efficiency
- ρ = density
- Δ = difference

Indices

- $'$ = isentropic process
- * = normalized value
- — = mean value
- 0 = stagnation property
- 1 = cycle start
- 2 = collector inlet
- 3 = turbine inlet
- 4 = chimney exit
- exp = expansion
- lim = limiting
- solar = solar power
- shaft = shaft power
- te = turbine exit
- turb = turbine
- z = vertical

Solar Collector

- E = emissivity
- G = radiation
- h = heat transfer coeff.
- H = heat flow into air
- K = conductivity
- L = thickness
- Q = heat flow in collector
- r = collector radius
- σ = Stefan-Boltzmann const.
- τ = transmissivity

Indices

- air = collector air
- atm = atmospheric air
- glass = glass properties
- gli = glass inner surface
- glo = glass outer surface
- Gro = ground properties
- in = inlet
- loss = heat loss
- out = outlet
- sto = ground storage
- surf = ground surface

References

[1] Trieb, F., Langniß, O., and Klaiß, H., 1997, ''Solar Electricity Generation—A Comparative View of Technologies, Costs and Environmental Impact,'' Sol. Energy, **59**, Nos. 1–3, pp. 89–99.

[2] Schlaich, J., 1995, ''The Solar Chimney: Electricity from the Sun,'' C. Maurer, Geislingen, Germany.

[3] Haaf, W., Friedrich, K., Mayr, G., and Schlaich, J., 1983, ''Solar Chimneys: Part I: Principle and Construction of the Pilot Plant in Manzanares,'' International Journal of Solar Energy, **2**, No. 1, pp. 3–20.

[4] Von Backström, T. W., and Gannon, A. J., 2000, ''The Solar Chimney Air Standard Cycle,'' South African Institution of Mechanical Engineering R&D Journal, **16**, March 2000, pp. 16–24.

[5] Cohen, H., Rogers, G. F. C., and Saravanamuttoo, H. I. H., 1996, *Gas Turbine Theory*, Fourth Edition, Addison Wesley Longman Limited, England, pp. 37–45.

[6] Von Backström, T. W., and Gannon, A. J., 2000, Compressible Flow Through Tall Chimneys, Proceedings of Solar 2000, Madison, Wisconsin, June 2000.

[7] Preston-Whyte, R. A., and Tyson, P. D., 1989, *The Atmosphere and Weather of Southern Africa*, Oxford University Press, Cape Town, South Africa.

[8] Incropera, F. P., and DeWitt, D. P., 1990, *Introduction to Heat Transfer*, John Wiley & Sons, Singapore.

[9] Holman, J. P., 1992, *Heat Transfer*, Seventh Edition, McGraw-Hill Book International (UK) Limited, London.

[10] Sears, F. W., Zemansky, M. W., and Young, H. D., 1987, *University Physics*, 7th Edition, Addison-Wesley Publishing Company, USA.

[11] Haaf, W., 1984, ''Solar Chimneys: Part II: Preliminary Test Results from the Manzanares Pilot Plant,'' International Journal of Solar Energy, **2**, No. 2, pp. 141–161.